J|A|C|S
COMMUNICATIONS

Published on Web 10/16/2007

Spectroscopic Evidence for a High-Spin Br-Fe(IV)-Oxo Intermediate in the α-Ketoglutarate-Dependent Halogenase CytC3 from *Streptomyces*

Danica Galonić Fujimori,[†] Eric W. Barr,[‡] Megan L. Matthews,[§] Gretchen M. Koch,[‡] J. Ryan Yonce,[||] Christopher T. Walsh,*[,†] J. Martin Bollinger, Jr.,*[,‡,§] Carsten Krebs,*[,‡,§] and Pamela J. Riggs-Gelasco*[,||]

Department of Biological Chemistry and Molecular Pharmacology, Harvard Medical School, Cambridge, Massachusetts 02115, Departments of Biochemistry and Molecular Biology and of Chemistry, The Pennsylvania State University, University Park, Pennsylvania 16802, and Department of Chemistry and Biochemistry, College of Charleston, Charleston, South Carolina 29424

Received August 27, 2007; E-mail: gelascop@cofc.edu; jmb21@psu.edu; ckrebs@psu.edu; christopher_walsh@hms.harvard.edu

The Fe(II)- and αKG[1]-dependent oxygenases are a functionally and mechanistically diverse family of enzymes that catalyze numerous biologically important reactions.[2−6] They activate oxygen at a mononuclear non-heme Fe(II) center, which is in most cases facially coordinated by a $(His)_2$/(Asp/Glu) triad,[7] to couple the decarboxylation of αKG to the oxidation of their substrates. In most cases, substrate oxidation entails hydroxylation of an unactivated carbon center. The key intermediate of the catalytic cycle is a Fe(IV)−oxo intermediate, which abstracts a hydrogen atom from the substrate.[8−10] Recently, a subclass of these enzymes capable of halogenating aliphatic carbon centers was identified.[11−13] These reactions occur during biosynthesis of various halogenated natural products. Amino acids thioesterified to the phosphopantetheinyl group of the thiolation domain serve as substrates for the halogenases. In addition to their catalysis of chlorination reactions, bromination has also been observed.[14] Key insight into the mechanism of the αKG-dependent halogenases came from the crystal structure of the halogenase SyrB2 from *Pseudomonas syringae*.[15] The structure of the resting enzyme revealed a halogen (Br or Cl) ligand to the iron center at the site normally occupied by the carboxylate ligand. This result led to the proposal that the reaction may proceed via a variant of the canonical mechanism of the αKG-dependent dioxygenases (Scheme 1). Key steps of the mechanism are C−H cleavage by a halo−Fe(IV)−oxo intermediate, followed by rebound of the halide atom to the substrate radical. We recently studied the chlorination reaction of L-Aba tethered to the thiolation domain CytC2, L-Aba-*S*-CytC2, by the halogenase CytC3 from *Streptomyces*.[16] The C−H-cleaving intermediate comprises two high-spin Fe(IV) complexes in equilibrium. Here, we show that the analogous reaction with bromide under otherwise identical conditions also yields an intermediate state comprising two high-spin Fe(IV) complexes, and we use freeze−quench Fe K-edge X-ray absorption spectroscopy to demonstrate that the intermediate possesses a Br−Fe(IV)−oxo group, validating the ligation of halogen to iron at this stage of the catalytic cycle.

Mössbauer spectra of a sample of the CytC3·Fe(II)·αKG·L-Aba-*S*-CytC2·Br^- complex that was reacted with O_2 for 2 s[17] are shown in Figure 1 as hashed marks. The zero-field spectrum can be simulated as a superposition of the experimental spectrum of the reactant complex (12%, green) and two quadrupole doublets with parameters typical of high-spin Fe(IV): $\delta = 0.23$ mm/s, $|\Delta E_Q| = 0.81$ mm/s (68%, blue) and $\delta = 0.31$ mm/s, $|\Delta E_Q| = 1.06$ mm/s (18%, red). These parameters are almost identical to those observed for the two Fe(IV) intermediates of CytC3 detected in the presence of chloride rather than bromide, in which case the two species are present in approximately equal amounts. By contrast, the species with smaller isomer shift predominates by ∼3.7/1 in the case of the bromo complexes.

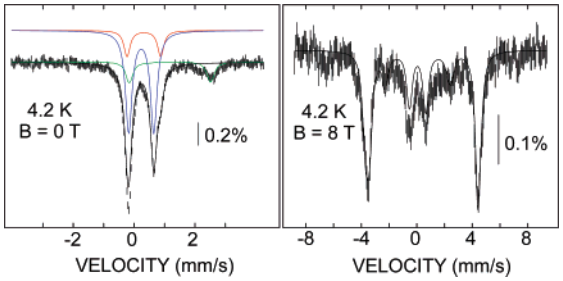

Figure 1. The 4.2-K Mössbauer spectra of a sample of the CytC3·Fe(II)·αKG·L-Aba-*S*-CytC2·Br^- complex that was reacted with O_2 for 2 s. The left panel shows the zero-field spectrum. The contribution of the reactant complex (12%) is shown in green. The remainder can be simulated with two quadrupole doublets representing the Fe(IV) intermediates with parameters given in the text. The right panel is the 8-T spectrum. The solid line is a spin-Hamiltonian simulation that assumes two high-spin Fe(IV) sites ($S = 2$, $D = 12.5$ cm^{-1}, $E/D = 0.05$) and uses the following parameters: $\delta = 0.23$ mm/s, $\Delta E_Q = -0.81$ mm/s, $\eta = -0.5$, $\mathbf{A}/g_N\beta_N = (-18.0, -18.0, -31.0)$ T (62%) and $\delta = 0.31$ mm/s, $\Delta E_Q = -1.06$ mm/s, $\eta = -0.5$, $\mathbf{A}/g_N\beta_N = (-18.0, -18.0, -31.0)$ T (18%).

Scheme 1. Proposed Mechanisms for Halogenation (R = $(CH_2)_2COO^-$; X = Halogen; R′H = T Domain-Bound Amino Acid)

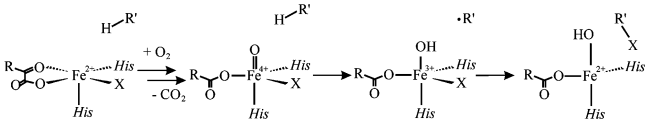

The 8-T spectrum reveals that the Fe(IV) intermediates are in the high-spin configuration, as was observed for all other Fe(IV) intermediates that have thus far been detected in the mononuclear non-heme-iron enzymes.[8,10,16,18] The spectrum was simulated under the assumption of slow relaxation with the spin Hamiltonian given in Supporting Information (SI) and the parameters given in the legend to Figure 1. Because the hyperfine tensors of related Fe(IV) intermediates are almost identical, $\mathbf{A}/g_N\beta_N = (-18, -18, -31)$ T,[19,20] this parameter was fixed for the analysis. With this assumption, the axial zero-field splitting parameter, D, was determined from the spectrum as $+12.5$ cm^{-1}, which is in the range typical of high-spin Fe(IV) intermediates.[10,16,19]

The high edge energy of the XANES spectrum of the Fe(IV) intermediate, shown in Figure 2, is consistent with the 86% Fe(IV): 14% Fe(II) reaction mixture (see SI). In addition, the area of the intermediate's 1s → 3d transition is substantially enhanced

[†] Harvard Medical School.
[‡] Department of Biochemistry and Molecular Biology, The Pennsylvania State University.
[§] Department of Chemistry, The Pennsylvania State University.
[||] College of Charleston.

10.1021/ja076454e CCC: $37.00

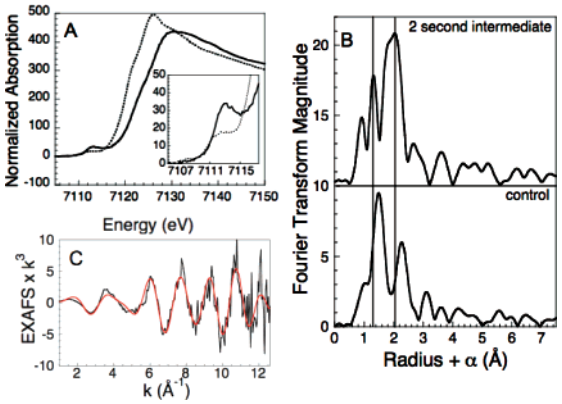

Figure 2. (A) XANES spectra of the CytC3·Fe(II)·αKG·L-Aba-*S*-CytC2·Br^- complex that was reacted with O_2 for 2 s (solid line) and anaerobic control (dashed line). (Inset) Pre-edge region. (B) FTs of the 2-s sample (top) compared to the anaerobic control (bottom). The vertical lines mark the oxo interaction and the bromo interaction. (C) A representative fit to unfiltered EXAFS data with 1.5 O at 1.87 Å (0.0017 $Å^2$), 2.5 O at 2.08 Å (0.0017 $Å^2$), 0.8 O at 1.61 Å (0.0016 $Å^2$), 0.8 Br at 2.43 Å (0.0036 $Å^2$) and 2 C at 3.09 Å (0.0021 $Å^2$).

relative to that of the anaerobic control. This enhancement is consistent with the asymmetry of the Fe-site imposed by the oxo ligand, as has been observed for TauD,[21] horseradish peroxidase,[22] and numerous model compounds.[23−25]

The FT of the EXAFS spectrum of the intermediate is shown in comparison to that of the control Fe(II) reactant in Figure 2. Both spectra have a prominent peak corresponding to the large bromine scatterer. In the control, the feature is best modeled with a single Fe−Br interaction at 2.53 Å, the same Fe−Br distance observed in the crystal structure of reduced SyrB2 in the presence of bromide.[15] In the spectrum of the 2-s sample, however, the peak is no longer resolved from the other first shell distances and is best modeled with a shorter Fe−Br distance of 2.43 Å, matching the Fe−Br distance found in a low-spin synthetic Br−Fe(IV)−oxo complex.[25] Fits that invoke chlorine or carbon as a scatterer instead of bromine either do not refine or are substantially worse than the bromine fits (see Tables S1 and S2 in SI for fitting details). The FT of the intermediate also has a peak corresponding to a very short first shell of ligands. Fits to both Fourier-filtered data and unfiltered data for the intermediate require a short Fe−oxygen interaction of 1.60−1.62 Å to best model the data. In addition, a shell of oxygens at 1.87−1.88 Å is also required, presumably corresponding to one or both of the oxygens in the bound succinate. The first coordination sphere is completed with a shell of longer Fe−O/N distances of 2.07−2.09 Å, most likely from the histidine ligands. Removal of either the oxo or bromine shell results in a substantially worse fit. When the coordination numbers of the bromine and oxo shells are incremented in 0.1 unit intervals for the best five-shell fit (which includes an outer carbon shell at 3.07−3.10 Å), the optimal coordination number is 0.8−1.0 for both shells, values that are consistent with the speciation determined by Mössbauer spectroscopy. The uncertainty of the coordination number does not allow us to address if both Fe(IV) species or only the predominate one has these structural features.

To conclude, the enhanced pre-edge feature in the Fe K-edge XAS spectra and the short Fe−O and Fe−Br interactions of 1.62 and 2.43 Å, respectively, support the formulation of this intermediate as a Br−Fe(IV)−oxo complex. The structural data provide further validation of the mechanism shown in Scheme 1, notably the direct coordination of the high-valent iron to halogen in preparation for oxidative transfer to substrate, and highlight the mechanistic similarities between the αKG-dependent dioxygenases and halogenases.

Acknowledgment. This work was supported by the NIH (Grants GM-20011 and GM-49338 to C.T.W., Grant GM-69657 to J.M.B. and C.K., and Grant NCRR-P20 RR-016461 to P.R.G.), the donors of the Petroleum Research Fund (Grant 41170-G3 to C.K.), the NSF (Grant MCB-642058 to J.M.B. and C.K.), the Beckman Foundation (Young Investigator Award to C.K.), the Dreyfus Foundation (Teacher Scholar Award to C.K.), and the Damon Runyon Foundation (Grant DRG-1893-05 for D.G.F.). Both the National Synchrotron Light Source and the Stanford Synchrotron Radiation Laboratory are national user facilities supported by the U.S. Department of Energy, Office of Basic Energy Sciences. The SSRL Structural Molecular Biology Program is supported by DOE and NIH-NCRR.

Supporting Information Available: Spin Hamiltonian used for simulation of the 8-T Mössbauer spectrum, a Mössbauer spectrum of the reaction product, details of the sample preparation and fitting analysis of the EXAFS data, additional edge and fit figures, and tables with the results of the analysis of the EXAFS data. This material is available free of charge via the Internet at http://pubs.acs.org.

References

(1) Abbreviations used: αKG, α-ketoglutarate; L-Aba, L-2-aminobutyric acid; TauD, taurine:α-ketoglutarate dioxygenase; XAS, X-ray absorption spectroscopy; XANES, X-ray absorption near edge spectrum; EXAFS, extended X-ray absorption fine structure; FT, Fourier transform.
(2) Solomon, E. I.; Brunold, T. C.; Davis, M. I.; Kemsley, J. N.; Lee, S.-K.; Lehnert, N.; Neese, F.; Skulan, A. J.; Yang, Y.-S.; Zhou, J. *Chem. Rev.* **2000**, *100*, 235−349.
(3) Costas, M.; Mehn, M. P.; Jensen, M. P.; Que, L., Jr. *Chem. Rev.* **2004**, *104*, 939−986.
(4) Hausinger, R. P. *Crit. Rev. Biochem. Mol. Biol.* **2004**, *39*, 21−68.
(5) Bollinger, J. M., Jr.; Price, J. C.; Hoffart, L. M.; Barr, E. W.; Krebs, C. *Eur. J. Inorg. Chem.* **2005**, *2005*, 4245−4254.
(6) Krebs, C.; Galonić Fujimori, D.; Walsh, C. T.; Bollinger, J. M., Jr. *Acc. Chem. Res.* **2007**, *40*, 484−492.
(7) Koehntop, K. D.; Emerson, J. P.; Que, L., Jr. *J. Biol. Inorg. Chem.* **2005**, *10*, 87−93.
(8) Price, J. C.; Barr, E. W.; Tirupati, B.; Bollinger, J. M., Jr.; Krebs, C. *Biochemistry* **2003**, *42*, 7497−7508.
(9) Price, J. C.; Barr, E. W.; Glass, T. E.; Krebs, C.; Bollinger, J. M., Jr. *J. Am. Chem. Soc.* **2003**, *125*, 13008−13009.
(10) Hoffart, L. M.; Barr, E. W.; Guyer, R. B.; Bollinger, J. M., Jr.; Krebs, C. *Proc. Natl. Acad. Sci., U.S.A.* **2006**, *103*, 14738−14743.
(11) Vaillancourt, F. H.; Yin, J.; Walsh, C. T. *Proc. Natl. Acad. Sci. U.S.A.* **2005**, *102*, 10111−10116.
(12) Vaillancourt, F. H.; Yeh, E.; Vosburg, D. A.; Garneau-Tsodikova, S.; Walsh, C. T. *Chem. Rev.* **2006**, *106*, 3364−3378.
(13) Galonić, D. P.; Vaillancourt, F. H.; Walsh, C. T. *J. Am. Chem. Soc.* **2006**, *128*, 3900−3901.
(14) Vaillancourt, F. H.; Vosburg, D. A.; Walsh, C. T. *ChemBioChem* **2006**, *7*, 748−752.
(15) Blasiak, L. C.; Vaillancourt, F. H.; Walsh, C. T.; Drennan, C. L. *Nature* **2006**, *440*, 368−371.
(16) Galonić, D. P.; Barr, E. W.; Walsh, C. T.; Bollinger, J. M., Jr.; Krebs, C. *Nat. Chem. Biol.* **2007**, *3*, 113−116.
(17) Final concentrations: 0.50 mM CytC3, 0.31 mM Fe, 2.4 mM αKG, 1.05 mM L-Aba-S-CytC2, 32 mM Br^-, and 1.26 mM O_2.
(18) Eser, B. E.; Barr, E. W.; Frantom, P. A.; Saleh, L.; Bollinger, J. M., Jr.; Krebs, C.; Fitzpatrick, P. F. *J. Am. Chem. Soc.* **2007**, *129*, 11334−11335.
(19) Krebs, C.; Price, J. C.; Baldwin, J.; Saleh, L.; Green, M. T.; Bollinger, J. M., Jr. *Inorg. Chem.* **2005**, *44*, 742−757.
(20) Sinnecker, S.; Svensen, N.; Barr, E. W.; Ye, S.; Bollinger, J. M., Jr.; Neese, F.; Krebs, C. *J. Am. Chem. Soc.* **2007**, *129*, 6168−6179.
(21) Riggs-Gelasco, P. J.; Price, J. C.; Guyer, R. B.; Brehm, J. H.; Barr, E. W.; Bollinger, J. M., Jr.; Krebs, C. *J. Am. Chem. Soc.* **2004**, *126*, 8108−8109.
(22) Penner-Hahn, J. E.; McMurry, T. J.; Renner, M.; Latos-Grazynsky, L.; Eble, K. S.; Davis, I. M.; Balch, A. L.; Groves, J. T.; Dawson, J. H.; Hodgson, K. O. *J. Biol. Chem.* **1983**, *258*, 12761−12764.
(23) Lim, M. H.; Rohde, J.-U.; Stubna, A.; Bukowski, M. R.; Costas, M.; Ho, R. Y. N.; Münck, E.; Nam, W.; Que, L., Jr. *Proc. Natl. Acad. Sci. U.S.A.* **2003**, *100*, 3665−3670.
(24) Rohde, J.-U.; Torelli, S.; Shan, X.; Lim, M. H.; Klinker, E. J.; Kaizer, J.; Chen, K.; Nam, W.; Que, L., Jr. *J. Am. Chem. Soc.* **2004**, *126*, 16750−16761.
(25) Rohde, J.-U.; Stubna, A.; Bominaar, E. L.; Münck, E.; Nam, W.; Que, L., Jr. *Inorg. Chem.* **2006**, *45*, 6435−6445.

JA076454E